# Short-Term and Seasonal Variability of the Atmospheric Water Vapor Transport through the Mackenzie River Basin

VLADIMIR V. SMIRNOV* AND G. W. K. MOORE

*Department of Physics, University of Toronto, Toronto, Ontario, Canada*

(Manuscript received 17 May 2000, in final form 14 October 2000)

ABSTRACT

The transport of water vapor through the Mackenzie River basin, a typical high-latitude river basin, is examined for the years 1979–93, with the European Centre for Medium-Range Weather Forecasts reanalysis dataset (ERA). It is shown that the transport of water vapor through the Mackenzie basin is highly variable in space and time. This transport has two distinct modes. During the autumn, winter, and spring, moisture is transported into the basin from the southwest by extratropical cyclones. The source of this moisture is argued to be the subtropical and midlatitude central Pacific Ocean. During the summer, moisture enters the basin from the northwest, with the source region being the Arctic Ocean. The values of monthly water vapor budgets obtained with the objectively analyzed fields are compared with those obtained from interpolated radiosonde data and with other known quantitative information about the water budget of the basin. It is found that the ERA data seriously overestimate the values of monthly water budget. A discussion of various potential sources of this discrepancy is provided.

## 1. Introduction

Studies of the hydrological cycle are extremely important for understanding the global climate system and its sensitivity to anthropogenic effects (Chahine 1992). Atmospheric water vapor is one of the major contributors to the greenhouse effect, to which the Arctic is most susceptible (Jones 1988; Manabe et al. 1991; Hinzman and Kane 1992). One of the regions that has experienced the greatest warming anywhere in the world over the last 30 years is the Mackenzie River basin (Cao et al. 2001). This makes the study of the atmospheric water vapor balance in this region particularly important.

Furthermore, the Mackenzie is the fourth largest river of the Arctic Ocean Basin. Its discharge, along with that of the other north flowing rivers, plays an important role in controlling the production of sea ice in the Arctic Ocean (Cattle 1985; Manak and Mysak 1989) and in regulating deep water formation in its marginal seas (Aagaard and Carmack 1989). The latter process is a key element of the thermohaline circulation of the world's oceans (Broecker 1991). The meteorological and hydrological processes that transport water into and through the high-latitude river basins are therefore of great importance to the entire climate research community.

The Mackenzie River basin (Fig. 1) covers an area of 1.787 million square kilometers, which is almost 20% of the Canadian landmass, and includes three large lakes, the eastern slopes of the Western Cordillera, and extensive wetlands. The typical yearly mean temperature is about 0°C; most of the ground is underlain by permafrost, and the river itself is frozen from November to June (Stewart et al. 1998). The mean annual precipitation in the Mackenzie basin is approximately 410 mm and varies from 300 mm in the eastern parts to 1600 mm on the slopes of the Rocky Mountains (Bjornsson et al. 1995; Stewart et al. 1998). Evaporation within the basin is estimated to be 100–200 mm $yr^{-1}$ from land and about 400 mm $yr^{-1}$ from water surfaces (Stewart et al. 1998).

Based on Water Survey of Canada data for the period 1973–93 from Arctic Red, a station near the mouth of the Mackenzie River, the mean annual discharge of the Mackenzie River into the Arctic Ocean is 288 $km^3$ (Stewart et al. 1998). It is interesting to note that this estimate of the mean annual discharge is 15% smaller than a previously and widely quoted estimate of 340 $km^3$ by Milliman and Meade (1983), which was based on data tabulated by UNESCO (1978). The reasons for this discrepancy are unclear but serve to highlight the uncertainty present in our knowledge of some of the

* V. V. Smirnov died in a mountain climbing accident in December 1999. This paper was completed after his death and is published as a memorial to him.

*Corresponding author address:* Dr. G. W. K. Moore, Dept. of Physics, University of Toronto, 60 St. George St., Toronto, ON M5S 1A7, Canada.
E-mail: moore@atmosp.physics.utoronto.ca

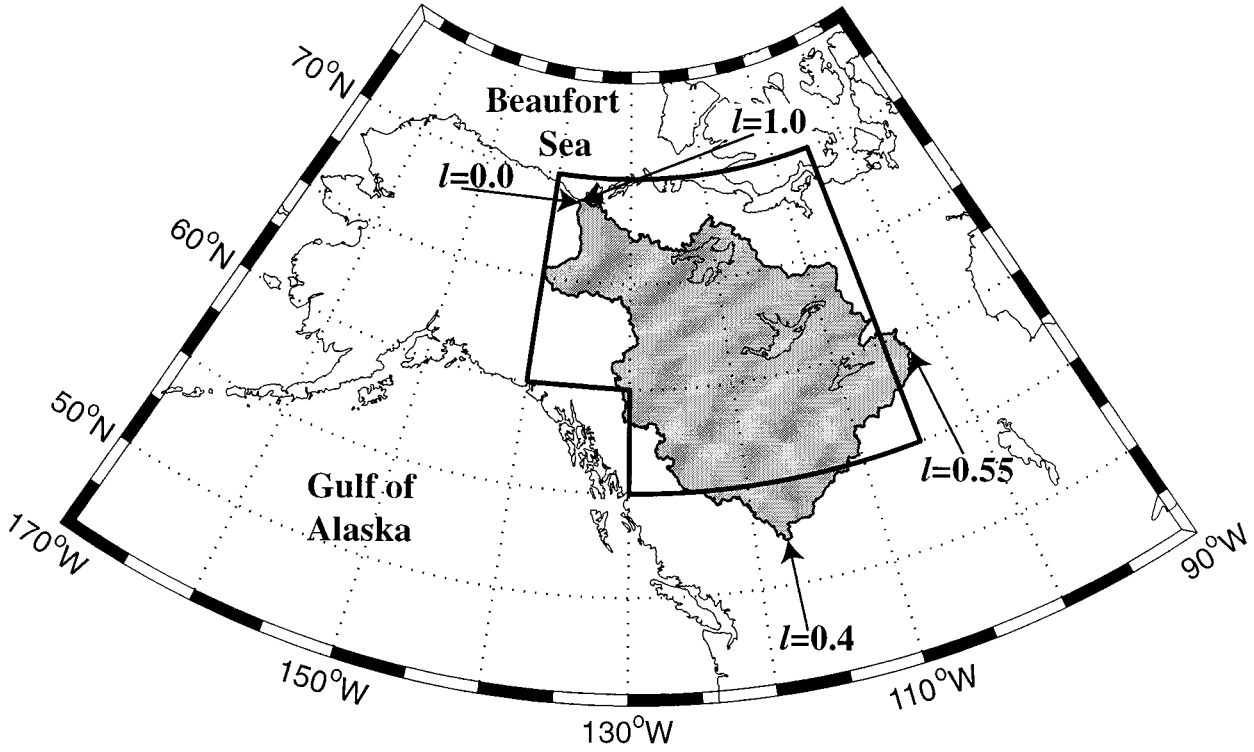


FIG. 1. A map of the Mackenzie River basin region. The shaded area is the actual area of the basin. The solid line is a polygonal approximation to the basin's boundary used by Walsh et al. (1994). The labels $l$ = (0.0, 0.4, 0.55, 1.0) refer to the locations on the basin's perimeter mentioned in Fig. 5.

most fundamental characteristics of the basin's water cycle.

The maximum precipitation, as well as maximum evaporation, occurs during summer months. However, the water budget of the basin (precipitation minus evaporation) has a minimum in summer (Walsh et al. 1994). According to Smirnov and Moore (1999), the transport of the water vapor through the Mackenzie basin is highly variable and is influenced by the occurrence and track of cyclones arriving from the North Pacific and Arctic Oceans. However, this conclusion was based on only 3 months of data and needs to be supported by more extensive studies.

Given the importance of the water vapor transport through the basin, there have been remarkably few studies that provide accurate quantitative information about it. The Mackenzie basin is now at the focus of the Canadian section of the Global Energy and Water Cycle Experiment (GEWEX), the international program to observe and model the moisture and energy fluxes in the atmosphere, the land surface, and the upper ocean. GEWEX is an integrated program of research and science activities ultimately leading to the prediction of global and regional climate change. Because Canada has the largest amount of freshwater in the world, the study of water resources and their variability from climate changes is the central goal of the Canadian contribution to GEWEX. The subprogram of GEWEX related to the Mackenzie basin is called the Mackenzie GEWEX Study (MAGS). Stewart et al. (1998) discusses the goals of MAGS in detail.

The studies of atmospheric moisture transport are often associated with the problem of the applicability of one or another source of data (e.g., Mo and Higgins 1996; Schmitz and Mullen 1996). Smirnov and Moore (1999) observe that, prior to 1996, most researchers preferred to use interpolated radiosonde data for atmospheric water vapor studies (e.g., Walsh et al. 1994; Serreze et al. 1995). Recently, both the the National Centers for Environmental Prediction (NCEP) and the European Centre for Medium-Range Forecasts (ECMWF) undertook major initiatives to use modern data assimilation algorithms to ''reanalyze'' all available historical datasets of meteorological state variables with the objective of producing time series of meteorological fields appropriate for short-term climate research and monitoring (Kalnay et al. 1996). The use of reanalysis data is especially appropriate for studies where radiosonde stations are sparse, such as is the case of the Mackenzie basin, and where data assimilation may produce better estimates of meteorological parameters than a simple spatial interpolation of sparse radiosonde data. On the other hand, the accuracy of the objective analyses may depend on the properties of the model and the region of interest, and these dependencies are not always well documented or understood. Therefore, an important

research focus is to find out how well the new reanalysis products represent regional high-latitude moisture transport.

Cullather et al. (2000) evaluated the atmospheric moisture budget over the Arctic Basin as depicted in both the NCEP and ECMWF reanalyses. For the moisture transport across 70°N, they find good agreement between the two products. A comparison with radiosonde data highlighted a problem with the latter's depiction of the summertime meridional moisture transport. Cullather et al. (2000) observe that the basin averaged precipitation minus evaporation/sublimation ($P - E$) field deduced from the convergence of the atmospheric moisture field of either reanalysis is significantly larger than that derived from the corresponding precipitation and evaporation fields. They note that the basin-averaged $P - E$ field calculated from the reanalyses' atmosphere moisture transport is in better agreement with previous studies. The nonclosure of the atmospheric moisture budget in either reanalysis was attributed to anomalously large evaporation. With regard to this last point, Renfrew et al. (2001) note a similar systematic error in the latent heat flux from the NCEP reanalysis over the Labrador Sea during winter. They attribute the error to the roughness length formula for moisture employed in the NCEP reanalyses that is inappropriate for use in high latitudes.

In this paper, the following issues are addressed. The water vapor flux fields over the Mackenzie basin, as calculated from the ECMWF reanalyses, are studied. The preliminary findings by Smirnov and Moore (1999) on short-term variability are supported by the evidence from 15 years of data. They are also extended to include seasons other than the autumn. The hypothesis that the Pacific Ocean is the major source of moisture in the Mackenzie basin (Bjornsson et al. 1995; Lackmann and Gyakum 1996; Lackmann et al. 1998) is again demonstrated, and the features of the spatial and temporal structure of the moisture transport are analyzed in detail. The seasonal changes in the transport are used to explain the known features of the basin's annual water cycle (Walsh et al. 1994). The discrepancies between our results, those of Walsh et al. (1994), and other estimates of the basin's water budget are discussed.

## 2. Analysis procedures and data

The equation describing the conservation of water vapor in an air column above a particular point of the earth's surface, if the flux across the upper boundary, diffusion, and liquid and solid phase transports are neglected, is

$$P - E = -\frac{\partial W}{\partial t} - \mathrm{div}\mathbf{Q}. \tag{1}$$

Here, $P$ is the precipitation rate, $E$ is the evaporation rate (both at the surface), $W$ is the precipitable water, defined by

$$W = \frac{1}{g}\int_0^{p_0} q\, dp, \tag{2}$$

and $\mathbf{Q}$ is the vertically integrated moisture flux:

$$\mathbf{Q} = \frac{1}{g}\int_0^{p_0} q\mathbf{v}\, dp. \tag{3}$$

In these formulas $q$ is specific humidity, $\mathbf{v}$ is the horizontal wind velocity, $p$ is the pressure, and $p_0$ is the surface pressure. The lower limit of integration can be set to zero or to any other level in the upper atmosphere above which the specific humidity can be neglected. In our calculations, the value of 100 hPa was chosen.

For long time intervals (1 month or more), the contribution of the div$\mathbf{Q}$ term is more significant than that of the precipitable water tendency (Walsh et al. 1994; Serreze et al. 1995). Indeed, averaging (1) over a long period of time yields

$$\overline{P} - \overline{E} = -\frac{\Delta W}{\Delta t} - \overline{\mathrm{div}\mathbf{Q}}, \tag{4}$$

where the first term on the right-hand side obviously approaches 0 as $\Delta t$ grows; for $\Delta t = 1$ month, it does not exceed 25% of the mean flux divergence in Arctic regions (Serreze et al. 1995). However, at smaller $\Delta t$ the precipitable water tendency in (4) does not need to be much smaller than the last term. Therefore, in short-term studies we cannot neglect it (Smirnov and Moore 1999).

The integration of (1) over the Mackenzie basin area $A$ yields

$$\iint_A (P - E)\, dA = -\frac{\partial}{\partial t}\iint_A W\, dA - \oint_{\partial A} (\mathbf{Q}, \mathbf{n})\, dl, \tag{5}$$

where $l$ is an element of the boundary $\partial A$ of the area $A$ and $\mathbf{n}$ is a normal to the basin. In what follows, the notation $\hat{Q} = -\oint_{\partial A} (\mathbf{Q}, \mathbf{n})\, dl$ will be used to denote the last term of (5). If, similar to (4), we average (5) over a period of time, it yields

$$\langle P\rangle - \langle E\rangle = -\langle w\rangle + \langle Q\rangle, \tag{6}$$

where $\langle P\rangle = \iint_A \overline{P}\, dA$, $\langle E\rangle = \iint_A \overline{E}\, dA$, $\langle w\rangle = \iint_A \Delta W/\Delta t\, dA$, $\langle Q\rangle = (1/\Delta t)\int_{\Delta t} \hat{Q}(t)\, dt$.

Walsh et al. (1994) were the first to give the estimates basin's water budget based on spatially interpolated radiosonde data over the period 1973–90. Figure 2 summarizes the results they obtained for the annual water cycle of the basin. Note that the integration was done not over the actual basin area, but over the simplified domain as shown in Fig. 1. The effect that this approximation has on the basin's water budget will be discussed below. We see that $\langle Q\rangle$ is responsible for most of the basin's moisture budget, and the contribution of the atmospheric storage term $\langle w\rangle$ is negligible. As discussed above, both the precipitation and evaporation are highest during the summer months. In contrast, $\langle Q\rangle$ is

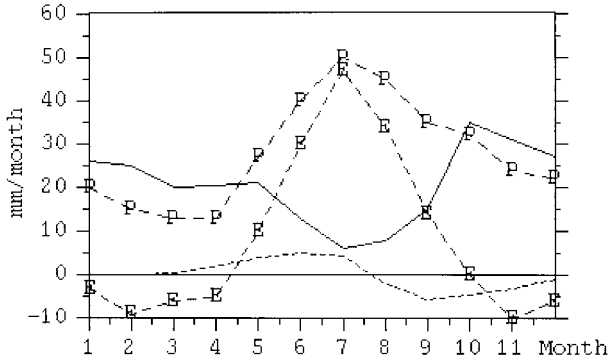


FIG. 2. Annual water cycle of the Mackenzie basin according to Walsh et al. (1994). The solid line is $\langle Q \rangle$, the line marked P is precipitation $\langle P \rangle$ based on measurements from 53 stations around the basin, the dotted line is $\langle w \rangle$, and the line E is the evaporation $\langle E \rangle$, which is determined as the residual of the other three terms.

a minimum during the summer months and attains its highest values in the autumn. The evaporation was determined as the residual of the other terms in (6). It can be seen to be negative during the winter months. This nonclosure of the moisture budget was attributed by Walsh et al. to errors in $\langle P \rangle$, specifically errors in measuring snowfall.

In this paper, we will use the ECMWF global reanalysis (ERA, Gibson et al. 1997) to characterize the atmospheric transport of moisture through the basin and its water budget. Standard surface and upper air fields are included in the reanalysis. The data are interpolated onto 11 standard pressure levels (1000, 925, 850, 700, 500, 400, 300, 250, 200, 150, and 100 hPa) and to the horizontal grid with a uniform 2.5° spacing. The vector **Q** is the primary source of diagnostics. It was calculated every 6 h using (3) over the 15-yr period from 1979 to 1993. For further information on particulars of the processing, please refer to Smirnov and Moore (1999).

## 3. Results and discussion

### *a. Short-term variability*

Figure 3 shows a time series of the vertically integrated atmospheric moisture flux $\hat{Q}$ through the basin for the Mackenzie basin during 1980. The year was chosen at random; other years show a similar pattern. We see that $\hat{Q}$ is characterized by a sequence of events with positive and negative values. From (5) it can be seen that a positive (negative) value of $\hat{Q}$ is associated with a net inflow (outflow) of atmospheric water vapor into the basin. Another important characteristic of the $\hat{Q}$ time series is that the instantaneous values are an order of magnitude larger than the monthly or annual means.

Further information on the characteristics and temporal variability of inflow and outflow events can be obtained if we define sets of inflow events for a given calendar month $\{t_i^{+S},\ i = 1, \ldots, N_{+S}\}$ that satisfy the following:

1) the event is one in which there is a net inflow of moisture, that is, $\hat{Q}(t_i^{+S}) > 0$;
2) the event is a local maximum, that is, $d\hat{Q}/dt|_{t=t_i^{+S}} = 0$; and
3) the magnitude of the inflow exceeds the monthly mean $\langle Q \rangle$ by an amount $S$, that is, $\hat{Q}(t_i^{+S}) - \langle Q \rangle > S$.

In the same manner, sets of outflow events $\{t_i^{-S},\ i = 1, \ldots, N_{-S}\}$ can be defined. If $\sigma$ is the standard deviation of $\hat{Q}(t)$ about the monthly mean, then $N_{+\sigma}$ and $N_{-\sigma}$ represent the number of events for a given calendar month for which there is strong inflow or outflow with magnitudes exceeding the monthly mean by $\sigma$. In a similar fashion, $N_{+2\sigma}$ and $N_{-2\sigma}$ are the number of inflow/outflow events with magnitudes exceeding the monthly mean by $2\sigma$.

Figure 4 shows the seasonal cycle in $N_{+\sigma}$, $N_{-\sigma}$, $N_{+2\sigma}$,

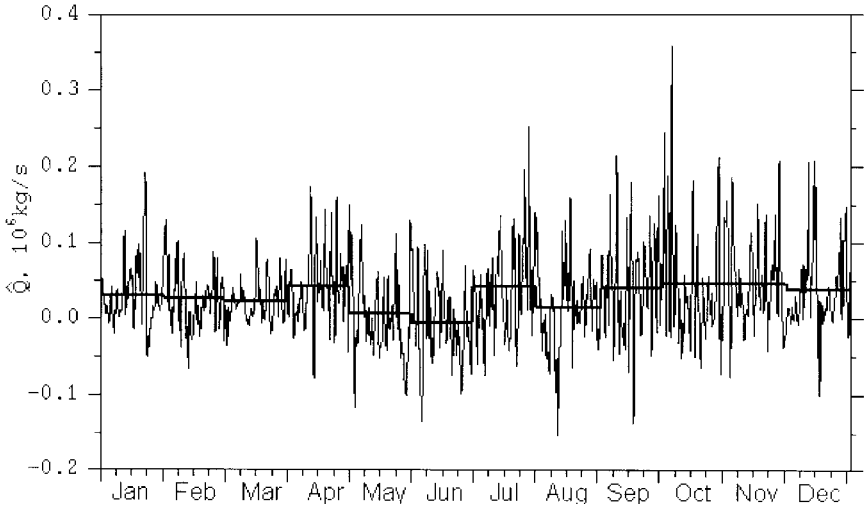


FIG. 3. Time series of $\hat{Q}(t)$ from the Mackenzie basin (mm month$^{-1}$) for 1980. The thick horizontal lines are the monthly means.

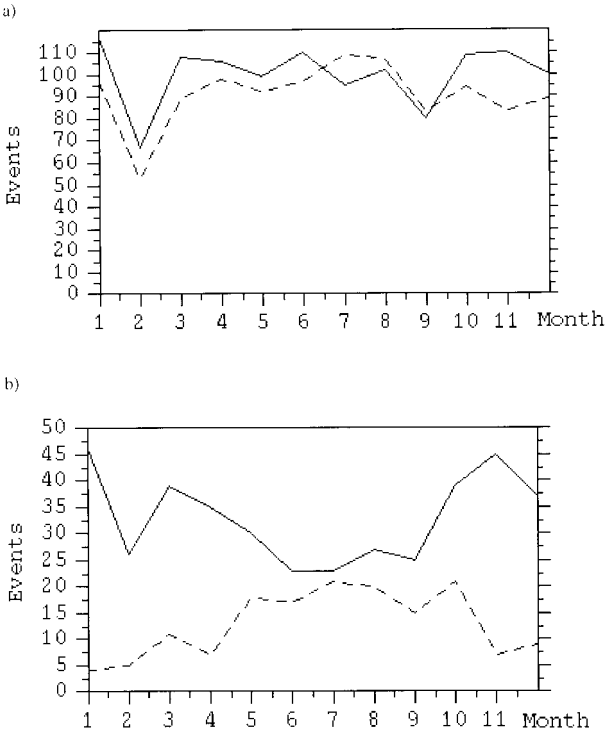


FIG. 4. The number of events with the magnitude of $\hat{Q}$ of more than (a) 1 standard deviation or (b) 2 standard deviations from the monthly means for 1979–93. Solid lines represent inflows; dashed lines represent outflows.

and $N_{-2\sigma}$ as calculated from the 15 yr of ERA data. We see that both $N_{+\sigma}$ and $N_{-\sigma}$ equal 80–110 events for each month over the 15 yr, which is equivalent to approximately 5–8 strong inflows and the same number of outflows per month every year. This confirms the visual observation from Fig. 3 that the moisture transport in the Mackenzie basin is a sequence of frequent strong inflows and outflows. The number of $2\sigma$ events is at least 30–50 per month over the 15 yr (equivalent to approximately 2–3 per month every year). Unlike $N_{\pm\sigma}$, there is a strong annual cycle in $N_{\pm 2\sigma}$. In winter months, there are numerous strong inflows and almost no outflows, while in summer, $N_{+2\sigma} \approx N_{-2\sigma}$. As we shall see, this fact will help to explain the characteristics of the basin's annual water cycle.

The preliminary results of Smirnov and Moore (1999) suggest that the transient events carrying moisture into the basin follow more or less the same track, forming a so-called atmospheric river. This definition was introduced by Zhu and Newell (1994) for filaments of increased moisture transport that exist for long periods of time (earlier as ''tropospheric rivers'' by Newell et al. 1992). Such filaments may be associated with cyclone tracks, with cyclones moving along the leading edge of the river.

Figure 5a shows the 15-yr mean zonal transport $Q_x$ through 130°W longitude (to the west of the Mackenzie basin). The band of large positive values between 45° and 55°N indicates the location of the atmospheric river that transports moisture into the basin from the southwest. During June–September, the axis of the atmospheric river shifts slightly northward and an additional weaker inflow from the northwest can be observed between 65° and 80°N. These two different patterns will hereinafter be referred to as winter and summer modes of the moisture transport. They were first detected by Smirnov and Moore (1999) in their study of 3 months (August–October 1994) of ECMWF operational analyses. In that year, the transition between summer and winter modes occurred in mid-September. The analysis of 15 yr of ERA data shows that these transitions occur almost every year, with one or two exceptions, typically in June (winter to summer mode) and September (summer to winter mode). Figure 5b shows a similar Hovmöller plot for 1982. It has the same general characteristics as in the 15-yr mean. However, the individual events that constitute the rivers can be identified. Figure 5c displays the magnitude of $Q_n$, the component of **Q** normal to the basin contour, for the same year as calculated by the method described by Smirnov and Moore (1999). Here we can see all individual events entering and exiting the basin. Areas of red denote inflows of moisture into the basin, and areas of blue indicate outflows. In confirmation with the resulted presented in Fig. 4, strong outflows of moisture are more common in summer.

### *b. Seasonal variability*

In Fig. 5 it can be seen that the atmospheric river shifts north in May–August—the months when the minimum of $P - E$ has been observed by Walsh et al. (1994) (see Fig. 2) and when most outflow events are observed (Fig. 4b). It is interesting to see the relationships between these three phenomena. We will do this by analyzing the monthly mean fields of moisture transport **Q** and geopotential height $Z$ at 700 hPa ($Z_{700}$) for selected months representing different stages of the annual cycle. January (Fig. 6a) is a typical month when the moisture transport is in its winter mode (all months between October and April show similar patterns). Figure 6b shows May, the month when the transition between winter and summer modes occurs. Fig. 6c shows July, a typical month during the summer mode.

Figure 6a gives us an idea of the geometry of the moisture flows and pressure fields during the period October–April (the ''winter mode'' of moisture transport observed in Fig. 5). In the beginning of this period, a climatological low, known as the Aleutian low (Haurwitz and Austin 1944) forms over the Gulf of Alaska, and persists until late April or even May. During this period, the atmospheric river exists to the south of this low, entering the Mackenzie basin from the southwest, as shown in Fig. 5c. An area of strong convergence of **Q** exists along the Western Cordillera that marks the western boundary of the basin. This area of convergence

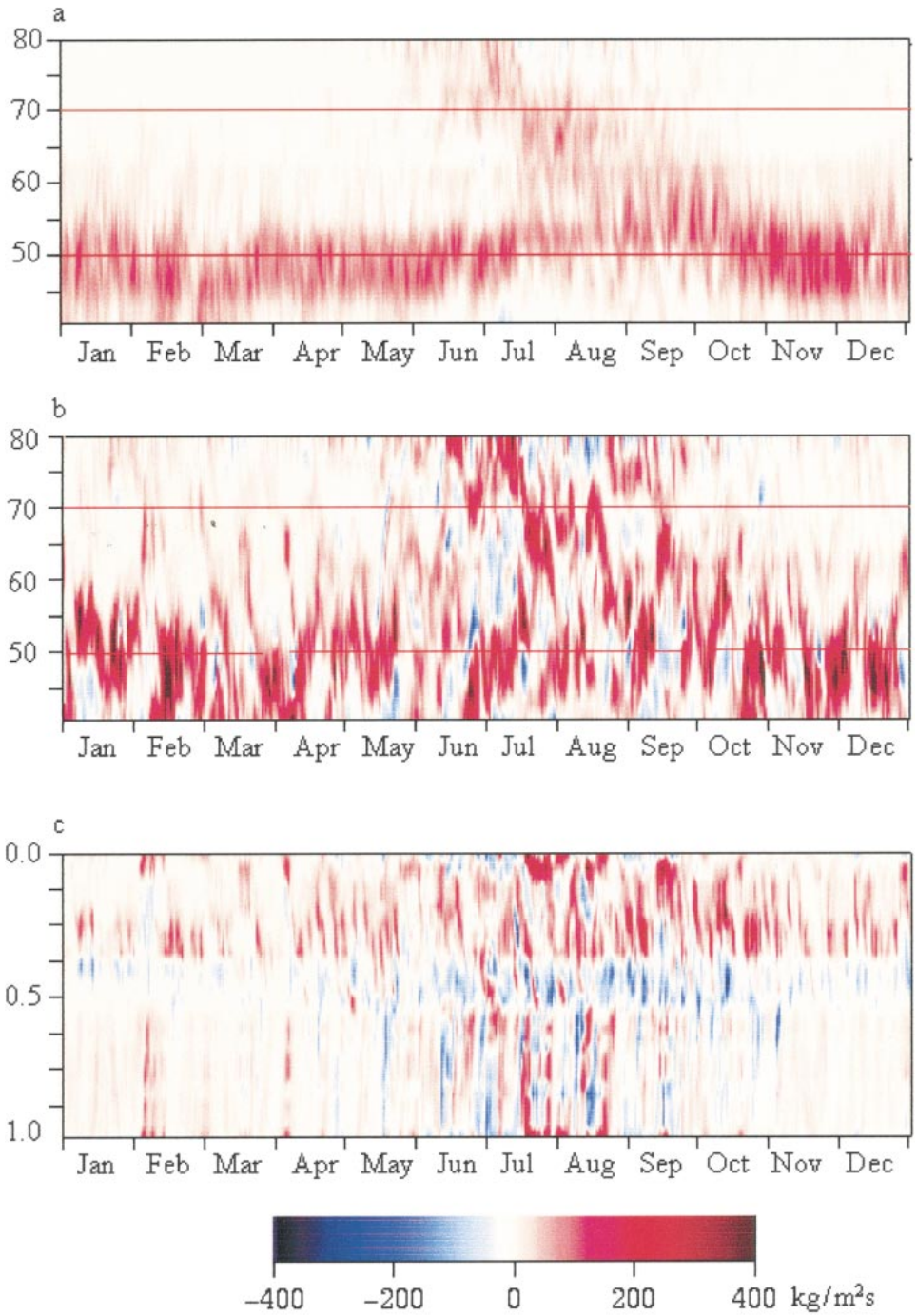


FIG. 5. Hovmöller plots of the zonal component of **Q** across 130°W (a) averaged for the 15-yr period of 1979–93 and (b) for 1982. The vertical axis is the latitude in degrees. The Mackenzie basin lies between latitudes 50° and 70°N (marked with red lines). Positive values represent eastward transport. (c) Hovmöller plot of $Q_n$ along the basin outline for 1982; the vertical axis is the basin contour $l$ in nondimensional units from 0 to 1 (see Fig. 1). Positive $Q_n$ corresponds to inflows of moisture into the basin, negative to outflows.

exists throughout the winter, gradually weakening in magnitude. By May (Fig. 6b), although the positions of the Aleutian low and atmospheric river have not changed, there is, however, no pronounced area of convergence to the southwest of the basin. In June–August (Fig. 6c), the Aleutian low weakens and we see the additional moisture flow in the northern parts of the basin. We also see strong flows of moisture exiting the basin, which corresponds to what was observed in Fig. 4b.

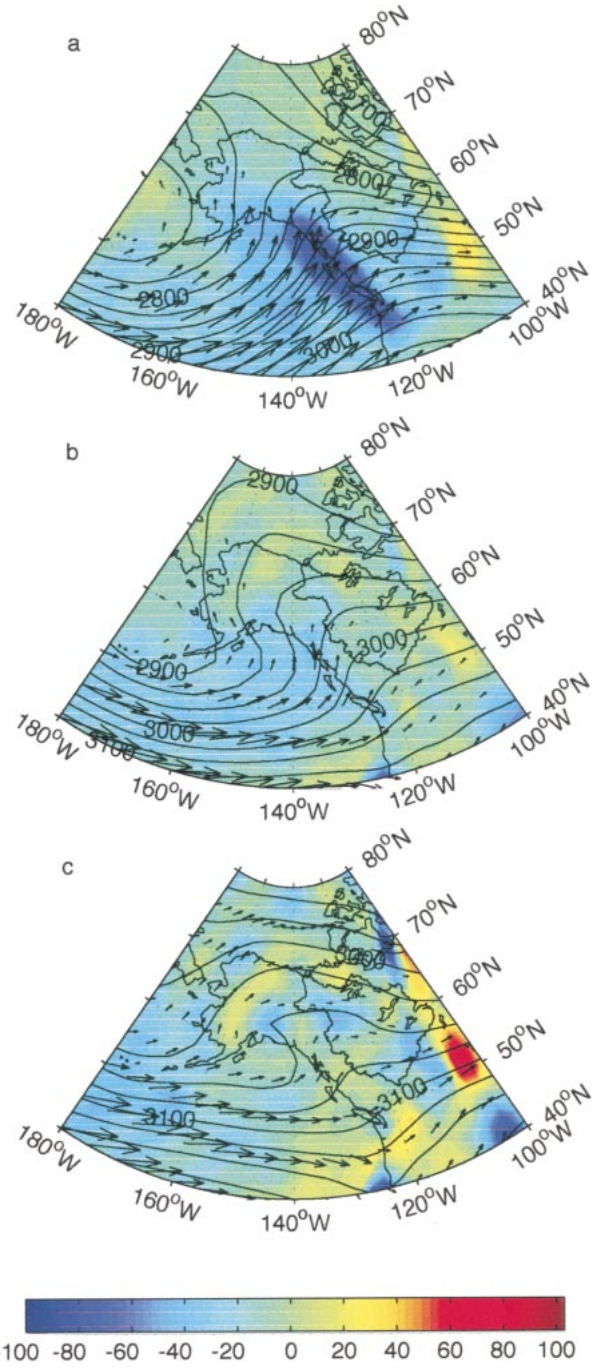


FIG. 6. Monthly mean **Q** (kg m$^{-2}$ s$^{-1}$; arrows), div**Q** ($10^{-5}$ kg m$^{-3}$ s$^{-1}$; shadings), and $Z_{700}$ (m; contours) for (a) Jan, (b) May, and (c) Jul. The maximum vector length is 200 kg m$^{-1}$ s$^{-1}$. Vectors below 20 kg m$^{-1}$ s$^{-1}$ are not shown.

Smirnov and Moore (1999) provided evidence that coherent atmospheric structures were responsible for moisture transport through the basin. With the 15 yr of data now available, we are in a position to confirm their conjectures. Figure 4 shows a clear seasonality in the number and intensity of the inflow/outflow events. We will therefore consider the changes in the structure of these events throughout the year. We will do this by compositing the fields of moisture transport **Q** and geopotential height $Z$ for times preceding or following the strong moisture inflow events. Let us consider the times $t_i^{+2\sigma}$ of $2\sigma$ inflow events within a given calendar month during the 15 yr under consideration. Then for any field $X(t)$, we can define a composite field $X_c(\tau) = [\Sigma_i X(t_i^{+2\sigma} + \tau) - \overline{X}]/N_{+2\sigma}$, where $\overline{X}$ is the mean value of $X$ for each month. Here, $X_c$ is the average difference between the field of $X$ at $\tau$ hours after inflows (or, if $\tau$ is negative, $\tau$ hours prior to inflows) and the mean field. The Student's $t$ test is used to assess the points at which this difference is statistically significant. In the following figures, only points with the absolute values of $t$ test greater than 1, approximately equivalent to 85% significance, are displayed (Fischer and Yates 1974). As we shall see, the composite fields are mutually consistent and pass this test over a large geographical region, providing one with additional evidence as to the statistical significance and physical relevance of the result.

Figure 7 shows the 15-yr composite January fields of $\mathbf{Q}_c$ and $(Z_{700})_c$ for several values of $\tau$. In Fig. 7a ($\tau$ = 0) we see that the most significant inflows during this period occur when there is a deep low (>100 m deeper than the monthly mean) over the Gulf of Alaska and a high pressure ridge along the northern Pacific coast of North America. This synoptic situation would normally result in the southwesterly flow into the basin. Associated with this flow is a transport of moisture into the basin. There is an area of convergence in $\mathbf{Q}_c$ along Western Cordillera, the western boundary of the basin.

In Figs. 7b and c we show the composites at $\tau$ = −24 and −48 h It can be seen that the events characterized by strong moisture inflow into the basin are associated with minima in $(Z_{700})_c$ that advance from subtropical central Pacific Ocean at approximately 35°N, 180°W to the location shown in Fig. 7a. There are significant fluxes of moisture that are being transported by the cyclonic circulation around these lows. This means that strong inflows of moisture during the winter season (a similar situation can be observed in October–April) are often caused by cyclones that propagate toward the basin from the abovementioned region in the central Pacific.

A very different situation occurs during the summer. Figure 8 displays the composite fields of $\mathbf{Q}_c$ and $(Z_{700})_c$ with $\tau$ = 0, −12, and −24 h for July. It shows that, during this month, the strongest moisture inflows arrive from northwest and are associated with lows over the Beaufort Sea. These lows are shallower than those that are responsible for moisture inflows in winter, carry less moisture, and have a shorter lifetime [there are no significant areas of $(Z_{700})_c$ for $\tau \leq -12$ h]. This result is in agreement with the observation of Smirnov and Moore (1999), who traced the trajectories of short-lived and quickly moving mesoscale lows traveling from the North Pacific to the Beaufort Sea in August 1994 and

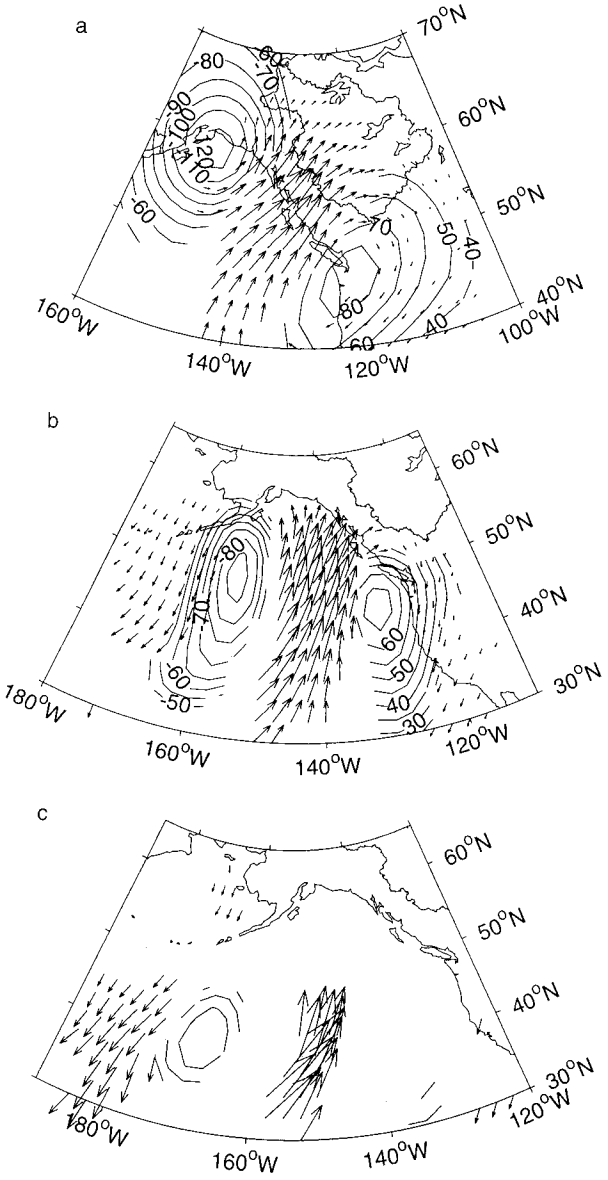


FIG. 7. Composite $\mathbf{Q}_c$ (kg m$^{-2}$ s$^{-1}$; arrows) and $(Z_{700})_c$ (m; contours) for Jan over the period of 1979–93 with (a) $\tau = 0$, (b) $\tau = -24$, and (c) $\tau = -48$ h. Note the change in domain in each panel. Only the statistically significant areas are displayed. The maximum vector length is 200 kg m$^{-1}$ s$^{-1}$.

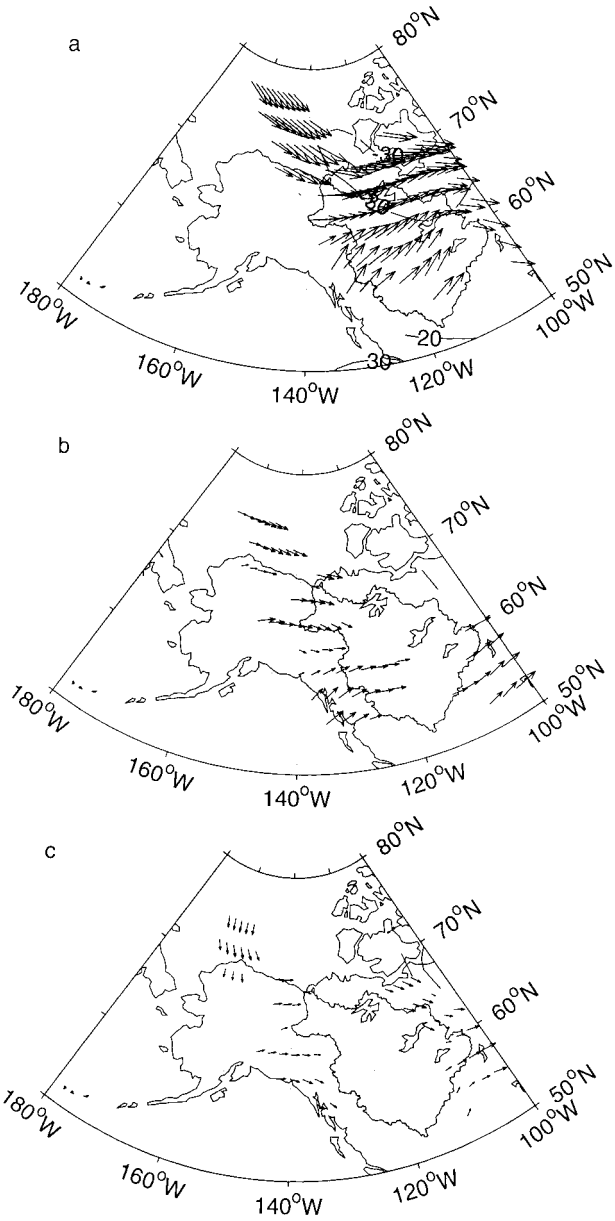


FIG. 8. Composite $\mathbf{Q}_c$ (kg m$^{-2}$ s$^{-1}$; arrows) and $(Z_{700})_c$ (m; contours) for Jul over the period of 1979–93 with (a) $\tau = 0$, (b) $\tau = -12$, and (c) $\tau = -24$ h. Only the statistically significant areas are displayed. The maximum vector length is 200 kg m$^{-1}$ s$^{-1}$.

identified them as sources of moisture for the Mackenzie basin. Similar systems can be observed in June–August. Asuma et al. (1998) describe in detail one such event that occurred in mid-September 1994.

It is equally interesting to see what follows the strong inflow events. Figure 9 shows the composite fields for January, May, and July with $\tau = +24$ h. It is apparent that an inflow must be followed by an outflow if the low system, or its remnant, reaches the eastern boundary of the basin. The question is how much of the moisture advected into the basin is simply advected out. In January, we can see a composite flow of moisture forming two areas of convergence in the basin, which suggests that most of the moisture associated with the $2\sigma$ inflow events stays in the basin as precipitation. Over the 24-h period between Fig. 7a and Fig. 9a, the low over the Gulf of Alaska was almost stationary. However, there is a composite low inside the basin, representing the secondary low development on the leeward side of the topography (Asuma et al. 1998; Mackay et al. 1998). In May and July (Figs. 9b and c), however, we don't see any significant convergence in $\mathbf{Q}_c$ (except for one

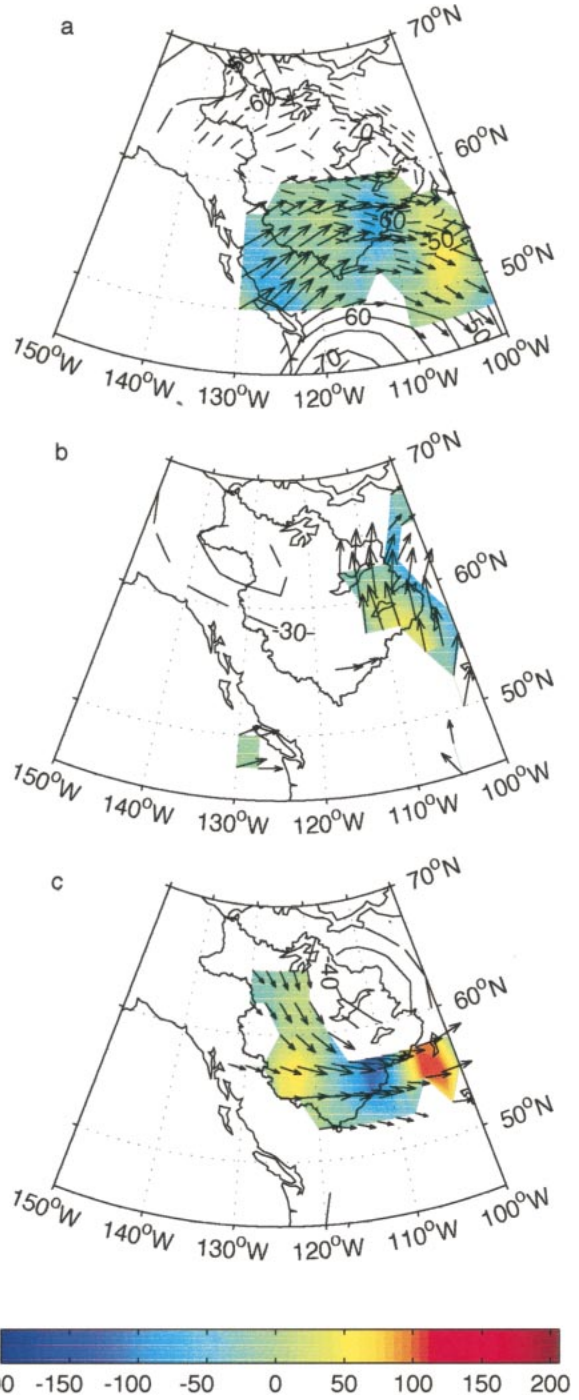


FIG. 9. Composite $\mathbf{Q}_c$ (kg m$^{-2}$ s$^{-1}$; arrows), div$\mathbf{Q}_c$ ($10^{-5}$ kg m$^{-3}$ s$^{-1}$; shadings), and $(Z_{700})_c$ (m; contours) at $\tau = +24$ h for (a) Jan, (b) May, and (c) Jul over the period of 1979–93. Only the statistically significant areas are displayed. The maximum vector length is 100 kg m$^{-1}$ s$^{-1}$.

area in Fig. 9c that will be discussed later). Moreover, there are areas of positive div$\mathbf{Q}_c$. This result means that most of the moisture associated with the inflow events is advected out of the basin. The reason for this difference may be the warmer air temperatures that allow evaporation from land. Therefore, we must expect that the net moisture budget in these months will be less than in January, and the strong outflows of moisture will be more numerous, as in Fig. 4b.

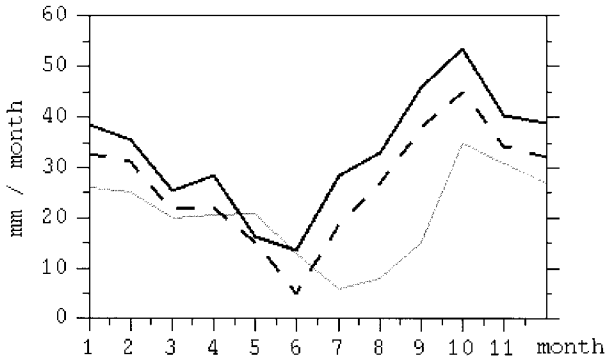


FIG. 10. Depictions of the annual water cycle over the Mackenzie basin. The thin solid line is the result of Walsh et al. (1994), the thick solid line is our result on the actual basin outline, and the dashed line is the result of ERA data integration on basin outline B (see Fig. 1).

Figure 10 displays the monthly mean moisture budgets according to Walsh et al. (1994) and those obtained from ERA data. Both annual cycle curves show a minimum in summer, as was suggested by the features of the ''summer mode'' described above. If we compare Figs. 4b and 10, it is apparent that the minimum $\langle Q \rangle$ occurs in the months with fewest inflow events and most outflow events.

The results described above suggest that individual inflow/outflow events play an important role in the basin's water budget. To quantify this, we will define the duration of an event at $t_i$ as $\{t_{i1} \le t_i \le t_{i2}\}$ where $t_{i1}$ and $t_{i2}$ are the start and end points of the event. They are taken as the times closest to $t_i$ at which either $\hat{Q}$ or $d\hat{Q}/dt$ is zero. For this event, the mass of water vapor transported in the basin is

$$m_i^+ = \int_{t_{i1}}^{t_{i2}} \hat{Q}\, dt.$$

For the set $\{t_i^{+S}\}$ defined above, $M^+ = \Sigma_{i=1,N_{+S}} m_i^+$ will be the contribution of these events to the monthly water vapor budget. Similarly, $M^-$ can be defined for the outflow events. Figure 11 shows the annual cycle of $M^+$ and $M^-$ for $S = \pm 2\sigma$. We can see that the $2\sigma$ inflow events contribute upward of 25%–50% of the total water vapor budget of the basin, even though there are only 2–3 of them per month on average. Meanwhile, the contribution of $2\sigma$ outflow events $M^-$ is between 5% in winter and 25% in summer.

As can be seen from Fig. 10, there are significant differences between the annual cycles obtained in this paper from the ERA data and that by Walsh et al. Most important is a significant difference in the magnitude of $\langle Q \rangle$. In addition, Walsh et al. have the minimum in $\langle Q \rangle$

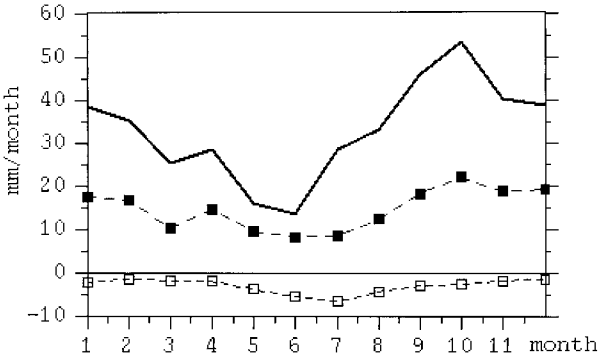


FIG. 11. The contribution of the inflow (black boxes) and outflow (white boxes) events to the basin's monthly moisture budgets (solid line) over the 15-yr period of 1979–93.

occurring in July–August, but the reanalysis data suggest that it occurs in May and June. Furthermore, the shape of the curve and the magnitude of $\langle Q \rangle$ depend on the definition of the Mackenzie basin outline. The reanalysis data integrated over the domain B used by Walsh et al. (see Fig. 1) are closer to their original result than when the Mackenzie basin is defined more accurately.

The mean annual water budget of the basin according to the ERA dataset is 398 mm $yr^{-1}$ for the exact basin and 325 mm $yr^{-1}$ for domain B, both of which are larger than the 249 mm $yr^{-1}$ quoted by Walsh et al. (1994). The first figure multiplied by the Mackenzie basin area gives 695 $km^3$ $yr^{-1}$. This value is more than double the actual value of the Mackenzie's discharge (between 280 and 340 $km^3$ $yr^{-1}$). These two quantities, annual water budget and annual discharge, should be equal over the 15-yr period under investigation, because the change of the atmospheric and ground water storage over this time period will be negligible. Thus, the magnitude of the total water vapor transport into the Mackenzie basin is strongly overestimated both by the ERA dataset and by Walsh et al. (1994).

The discrepancies among our results, the results of Walsh et al. (1994), and other estimates of the basin water budget may have several sources: 1) the different definitions of the Mackenzie basin's outline (see Fig. 10: the summer minimum becomes much deeper for the ''rectangular'' basin), 2) the fact that time period under consideration by Walsh et al. was different from that in this study (however, given the large degree of overlap between the two time periods, it is unlikely that this is the source of the discrepancy), and/or 3) the possibility that either the reanalysis fields used in this paper or the radiosonde data interpolation used by Walsh et al. fail to represent properly the transport of moisture through the basin.

With regard to this latter point, let us return to Fig. 6c. A dipole-like structure in the div**Q** field is present at 50°–60°N and 110°–100°W. A similar dipole can be observed in the composite moisture flux field in Fig. 9c. In both instances, there is a region of convergence of moisture flux over the eastern area of the basin. There is no physical reason for the existence of this dipole, and its presence may contribute to the overestimation of the basin's water budget. Indeed a simple ''adjustment'' of $\langle Q \rangle$ over the eastern section during the summer months, by setting it equal on an area-adjusted basis to that in the basin's central section, results in a mean annual water budget, on the Walsh et al. domain, of 280 mm $yr^{-1}$.

In addition, it is useful to remember that the grid spacing of the ERA data is only 2.5°. As was shown by Smirnov and Moore (1999), the error estimate for $\hat{Q}$ is

$$\frac{\Delta\hat{Q}}{\hat{Q}} \approx 2 \times 10^{-6} D\sqrt{N}\frac{\Delta Q}{Q},$$

where $D$ is the grid spacing in meters, $N$ is the number of data points on the basin's boundary (if we assume it is rectangular), and $\Delta Q/Q$ is the fractional error in the values of **Q** (which is mostly due to the overestimation of the midlevel humidity). In our case, $N = 41$, $D = 2.75 \times 10^5$ m in the meridional direction and half as much in zonal direction, so $\Delta\hat{Q}/\hat{Q} \approx 2.5\Delta Q/Q$. We do not know the values of $\Delta Q/Q$ for the ERA data; however, for the operational ECMWF objective analysis data, Smirnov and Moore (1999) estimate that it may be as high as 20% in the Mackenzie basin area. This would result in a 50% error for $\langle Q \rangle$. One manifestation of this error is an incorrect representation of the location and extent of the region of moisture flux convergence on the western boundary of the basin. This source of error also must be taken into account.

## 4. Summary

This paper describes the features of short-term and seasonal variability of the atmospheric water vapor transport through the Mackenzie River basin for 1979–93, based on the ECMWF reanalysis (ERA) data. The following important conclusions can be drawn from this work.

1) Structures similar to those described by Zhu and Newell (1994) as ''atmospheric rivers'' have been identified over the Mackenzie River basin for most of the period under consideration. These structures consist of sequences of moisture pulses coming into the Mackenzie basin from the southwest or northwest, carried by low pressure systems that have their origin over the Pacific Ocean or the Beaufort Sea. The moisture transport is highly variable in time. There are 5–8 events of each sign per month with the values of integrated moisture transport $\langle Q \rangle$ one standard deviation away from the monthly means, and 2–3 events that are two standard deviations away. It is shown that the latter events contribute to 25%–50% of the total water vapor budget of the basin. It is therefore important that the structure, evolution, and track of extratropical cyclones be accu-

rately represented if the transport of moisture into and through the basin is to be similarly represented.

2) The moisture transport has two distinct modes. The winter mode lasts from October through April. During this time, the moisture is advected into the basin from the southwest by cyclonic events originating in subtropical or midlatitude central Pacific. During the summer mode (June–August), the moisture pulses arrive from two directions: from the southwest, as in winter, and from the northwest, carried by synoptic-scale lows from the Arctic Ocean. The analysis of the composite fields of **Q** suggests that the strongest pulses of moisture in the summer mode arrive from the northwest. May and September are the typical months for the transition from one mode to the other. Therefore, the source of moisture for the Mackenzie basin appears to be the subtropical Pacific Ocean in winter and the Arctic Ocean in summer.

3) There is a discrepancy between the annual cycle of monthly moisture budgets as presented by Walsh et al. (1994) and as calculated from the ECMWF reanalyses. The problem is most acute during the summer months. Recently Cullather et al. (2000) have identified a similar failure in the representation of summer moisture transport over the Arctic Basin as represented in interpolated radiosonde data. In addition, the annual water budgets of the basin in both these estimates are about 100% larger than the actual discharge of the Mackenzie. Possible sources of this discrepancy include an underestimation of the evaporation (by at least 10 mm month$^{-1}$). This underestimation is most pronounced in the eastern part of the basin, where the field of div**Q** is obviously noisy and unphysical in July–October. In addition, there is evidence of an incorrect assessment of upper-level humidity fields in objective analysis data (Smirnov and Moore 1999). There is also the potential for significant errors that arise from the relatively coarse resolution of the ERA fields.

*Acknowledgments.* We express our gratitude to the National Center of Atmospheric Research (NCAR) for providing the ECMWF datasets and the Natural Science and Engineering Research Council (NSERC) for funding the project. Also, we thank I. Stern of NCAR and R. Crawford of Environment Canada for their invaluable help in data processing, and we thank Muyin Wang of Dalhousie University for comments and discussion. The insightful comments of the reviewers are also acknowledged.

## REFERENCES

Aagaard, K., and E. C. Carmack, 1989: The role of sea ice and other fresh water in the Arctic circulation. *J. Geophys. Res.,* **94,** 14 485–14 498.

Asuma, Y., S. Iwata, K. Kikuchi, G. W. K. Moore, R. Kimura, and K. Tsuboki, 1998: Precipitation features observed by Doppler radar at Tuktoyaktuk, NWT, Canada, during the Beaufort and Arctic Storms Experiment. *Mon. Wea. Rev.,* **126,** 2384–2405.

Bjornsson, H., L. A. Mysak, and R. D. Brown, 1995: On the interannual variability of precipitation and runoff in the Mackenzie drainage basin. *Climate Dyn.,* **12,** 67–76.

Blackmon, M. L., 1977: An observational study of the Northern Hemisphere winter time circulation. *J. Atmos. Sci.,* **34,** 1040–1053.

Broecker, W. S., 1991: The great ocean conveyor. *Oceanography,* **4,** 79–84.

Cao, Z., R. E. Stewart, and W. Hogg, 2001: Extreme winter warming events over the Mackenzie basin: Dynamic and thermodynamic contributions. *J. Meteor. Soc. Japan,* in press.

Cattle, H., 1985: Diverting Soviet rivers: Some possible repercussions for the Arctic Ocean. *Polar Rec.,* **22,** 485–498.

Chahine, M. T., 1992: The hydrological cycle and its influence on climate. *Nature,* **359,** 373–380.

Cullather, R. I., D. H. Bromwich, and M. C. Serreze, 2000: The atmospheric hydrologic cycle over the Arctic basin from reanalyses. Part I: Comparison with observations and previous studies. *J. Climate,* **13,** 923–937.

Fischer, R. A. and F. Yates, 1974: *Statistical Tables for Biological, Agricultural and Medical Research.* Longman Group, 146 pp.

Gibson, J. K., P. Kallberg, S. Uppala, A Hernandez, A. Nomura, and E. Serrano, 1997: ERA description. ECMWF Re-Analysis Project Rep. Series 1, 72 pp. [Available from ECMWF, Shinfield Park, Reading RG2 9AX, United Kingdom.]

Haurwitz, B., and J. M. Austin, 1944: *Climatology.* 1st ed. McGraw-Hill, 410 pp.

Hinzman, L. D., and D. L. Kane, 1992: Potential response of an Arctic watershed during a period of global warming. *J. Geophys. Res.,* **97,** 2811–2820.

Jones, P. D., 1988: Hemispheric surface air temperature variations: Recent trends and an update to 1987. *J. Climate,* **1,** 654–660.

Kalnay, E., and Coauthors, 1996: The NCEP/NCAR 40-Year Reanalysis Project. *Bull. Amer. Meteor. Soc.,* **77,** 437–471.

Lackmann, G. M., and J. R. Gyakum, 1996: The synoptic and planetary-scale signatures of precipitating systems over the Mackenzie River basin. *Atmos.–Ocean,* **34,** 647–674.

——, ——, and R. Benoit, 1998: Moisture transport diagnosis of a wintertime precipitation event in the Mackenzie River basin. *Mon. Wea. Rev.,* **126,** 668–91.

Mackay, M. D., R. E. Stewart, and G. Bergeron, 1998: Downscaling the hydrological cycle in the Mackenzie basin with the Canadian Regional Climate Model. *Atmos.–Ocean,* **36,** 179–211.

Manabe, S., R. J. Stouffer, M. J. Spelman, and K. Bryan, 1991: Transient response of a coupled ocean–atmosphere model to gradual changes in atmospheric $CO_2$. Part 1: Annual mean response. *J. Climate,* **4,** 785–818.

Manak, D. K., and L. A. Mysak, 1989: On the relationship between Arctic sea ice anomalies and fluctuations in northern Canadian air temperature and river discharge. *Atmos.–Ocean,* **27,** 682–691.

Milliman, J. D., and R. H. Meade, 1983: World-wide delivery of river sediment to the oceans. *J. Geol.,* **91,** 1–21.

Mo, K. C., and R. W. Higgins, 1996: Large-scale atmospheric moisture transport as evaluated in the NCEP/NCAR and the NASA/DAO reanalyses. *J. Climate,* **9,** 1531–1545.

Newell, R. E., N. E. Newell, Y. Zhu, and C. Scott, 1992: Tropospheric rivers? A pilot study. *Geophys. Res. Lett.,* **19,** 2401–2404.

Renfrew, I. A., G. W. K. Moore, P. S. Guest, and K. Bumke, 2001: A comparison of surface-layer and surface turbulent-flux observations over the Labrador Sea with ECMWF analyses and NCEP reanalyses. *J. Phys. Oceanogr.,* in press.

Schmitz, J. T., and S. L. Mullen, 1996: Water vapor transport associated with the summertime North American monsoon as depicted by ECMWF analyses. *J. Climate,* **9,** 1621–1634.

Serreze, M. C., R. G. Barry, and J. E. Walsh, 1995: Atmospheric water vapor characteristics at 70°N. *J. Climate,* **8,** 719–731.

Smirnov, V., and G. W. K. Moore, 1999: Spatial and temporal structure of atmospheric water vapor transport in the Mackenzie River basin. *J. Climate,* **12,** 681–696.

Stewart, R. E., and Coauthors, 1998: The Mackenzie GEWEX Study: The water and energy cycles of a major North American river basin. *Bull. Amer. Meteor. Soc.,* **79,** 2665–2683.

UNESCO, 1978: World Water Balance and Water Resources of the Earth. Studies and Reports in Hydrology, No. 25.

Walsh, J. E., X. Zhou, D. Portis, and M. C. Serreze, 1994: Atmospheric contribution to hydrologic variations in the Arctic. *Atmos.–Ocean,* **32,** 733–755.

Zhu, Y., and R. E. Newell, 1994: Atmospheric rivers and bombs. *Geophys. Res. Lett.,* **21,** 1999–2002.